

REALISTIC CALCULATIONS OF ONE- AND TWO-HADRON EMISSION PROCESSES OFF FEW- AND MANY-BODY NUCLEI*

M. Alvioli, C.Ciofi degli Atti, and L.P. Kaptari[†]

*Department of Physics, University of Perugia
and Istituto Nazionale di Fisica Nucleare,
Sezione di Perugia, Via A. Pascoli, I-06100, Italy*

H. Morita

Sapporo Gakuin University, Bunkyo-dai 11, Ebetsu 069, Hokkaido, Japan

Abstract

The exclusive electro-disintegration processes ${}^2\text{H}(e, e'p)n$, ${}^3\text{He}(e, e'p){}^2\text{H}$, ${}^3\text{He}(e, e'p)pn$, ${}^3\text{He}(e, e'pp)n$ and ${}^4\text{He}(e, e'p){}^3\text{H}$ have been calculated using realistic few-body wave functions and treating final state interaction (FSI) effects within a generalized eikonal approach. The semi-inclusive scattering $A(e, e'p)X$ off complex nuclei has been analyzed using many-body wave functions for ${}^{16}\text{O}$ and ${}^{40}\text{Ca}$, obtained within the framework of a linked cluster expansion and taking FSI into account by a Glauber-type approach. The effect of color transparency has also been included by considering the Finite Formation Time (FFT) that the hit hadron needs to reach its asymptotic physical state.

* Presented at the 6th International Workshop on "Electromagnetically Induced Two-Hadron Emission", Pavia, September 24-27, 2003

[†] On leave from Bogoliubov Lab. Theor. Phys.,141980, JINR, Dubna, Russia

I. INTRODUCTION

One of the main aims of nowadays hadronic physics is the investigation of the limits of validity of the so called *Standard Model* of nuclei, i.e. the description of nuclei in terms of the solution of the non relativistic Schrödinger equation containing realistic nucleon-nucleon interactions. To this end, exclusive lepton scattering could be very useful for it might yield relevant information on the nuclear wave function, provided the initial and final states involved in the scattering process are described within a consistent, reliable approach. In the case of *few-body systems*, a consistent treatment of initial and final states is nowadays possible at low energies (see e.g. [1, 2] and References therein quoted), but at high energies, when the number of partial waves sharply increases and nucleon excitations can occur, the Schrödinger approach becomes impractical and other methods have to be employed. In the case of *complex nuclei*, additional difficulties arise due to the approximations which are still necessary to solve the many-body problem. As a matter of fact, in spite of the fundamental progress made in recent years in the calculation of the properties of light nuclei (see e.g. [3]), much remains to be done, also in view that the results of very sophisticated calculations (*e.g.* the variational Monte Carlo ones [4]), show that the wave function which minimizes the expectation value of the Hamiltonian, provides a very poor nuclear density; moreover, the structure of the best trial wave function is so complicated, that its application to the calculation of various processes at intermediate and high energies, where the role of the so called *nuclear effects* is becoming more and more visible, appears to be not easy task. The aim of this talk is to summarize the activity carried out by the Perugia group in the field of the theoretical treatment of exclusive and semi-exclusive lepton scattering off both few- and many-nucleon systems. In the former case, *exact* realistic few-body wave functions have been used, whereas in the latter case, *reasonable* realistic many-body wave functions obtained from a cluster expansion calculation of the ground state energy, have been employed; these wave functions, which explain *reasonably* well the ground state energy, density and momentum distributions of complex nuclei, have, at the same time, a structure such that their application to various scattering problems is rather straightforward. The structure of the paper is as follows: in Section II few-body nuclei (2H , 3He and 4He) are discussed giving in Section II A the basic formulae for the calculations of the exclusive $A(e, e'p)B$ and $A(e, e'pp)C$ processes; in Section II B the numerical results for the processes

${}^2H(e, e'p)n$, ${}^3He(e, e'p)^2H$, ${}^3He(e, e'p)(pn)$ and ${}^4He(e, e'p)^3H$, treating the effects of the final state interaction (FSI) by a generalized eikonal approach, and also considering color transparency effects, are presented. In Section III complex nuclei are discussed: the basic formalism of the cluster expansion technique is illustrated in Section III A where the results of calculations for the ground-state energy, density and momentum distributions are presented; the effects of FSI in $(e, e'p)$ processes off complex nuclei is discussed in Section III B in terms of a generalized Glauber approach; the color transparency effects are introduced in Section III C; eventually, in Section IV the Conclusion are drawn.

II. FEW-BODY NUCLEI (Refs. [5–11])

A. Basic formulae

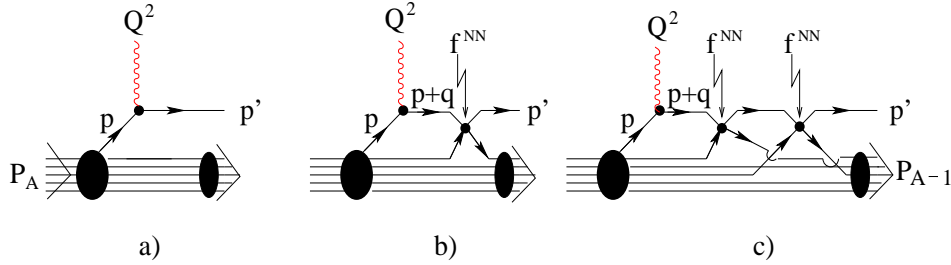


FIG. 1: The Feynman diagrams for the process $A(e, e'p)(A-1)$: the Plane Wave Impulse Approximation (PWIA) a), and the single b) and double c) rescattering in the final state. f^{NN} denotes the elastic nucleon-nucleon (NN) scattering amplitude.

In the one-photon-exchange approximation we write the differential cross section of the process $A(e, e'p)(A-1)$ in the following form

$$\frac{d^6\sigma}{dE_{e'}d\Omega_{e'}d\mathbf{p}_m} = K(x, Q^2, \mathbf{p}_m) \sigma_{cc1}^{eN}(Q^2, \mathbf{p}_m) |T_{A,A-1}(\mathbf{p}_m, E_m)|^2, \quad (1)$$

where $K(x, Q^2, \mathbf{p}_m)$ is a kinematical factor, $\sigma_{cc1}^{eN}(Q^2, \mathbf{p}_m)$ the De Forest CC1 cross section [12], $\mathbf{p}_m \equiv \mathbf{q} - \mathbf{p}'$ the *missing momentum*, i.e. the Center-of-Mass momentum of the undetected particles, \mathbf{p}' the momentum of the detected proton, and $E_m = \sqrt{P_{A-1}^2} + M_N - M_A = q_0 - T_{p'} - T_{A-1}$ the *missing (or removal) energy*.

In our approach the nuclear transition matrix element $T_{A,A-1}(\mathbf{p}_m, E_m)$ in eq. (1) is computed by evaluating the corresponding Feynman diagrams of Fig. 1, describing the interaction of the incident electron with one nucleon of the target followed by its elastic rescattering with the nucleons of the $(A - 1)$ nucleus.

B. Results of calculations

The process ${}^2H(e, e'p)n$

In PWIA the square of the transition matrix element in eq. (1) simply becomes the deuteron momentum distribution, i.e.

$$|T_{A,A-1}|^2 \rightarrow n_D(|\mathbf{p}_m|) = \frac{1}{3} \frac{1}{(2\pi)^3} \sum_{\mathcal{M}_D} \left| \int d\mathbf{r} \Psi_{1,\mathcal{M}_D}(\mathbf{r}) \chi_f \exp(-i\mathbf{p}_m \mathbf{r}) \right|^2 \quad (2)$$

where $\Psi_{1,\mathcal{M}_D}(\mathbf{r})$ is the realistic (containing S and D waves) deuteron wave function, and the missing momentum $\mathbf{p}_m = -\mathbf{p}$ is nothing but the inverse of the momentum of the bound proton (cf. Fig 1a)). When the FSI is taken into account, $\mathbf{p}_m \neq -\mathbf{p}$ and the final state of the (np) pair should be described by the solution of the Schrödinger equation in the continuum. When the relative energy of the (np) pair is large, the two-nucleon continuum wave function can be approximated by its eikonal form, obtaining [6]

$$n_D \rightarrow N_{eff}(\mathbf{p}_m) = \frac{1}{3} \frac{1}{(2\pi)^3} \sum_{\mathcal{M}_D} \left| \int d\mathbf{r} \Psi_{1,\mathcal{M}_D}(\mathbf{r}) \mathcal{S}(\mathbf{r}) \chi_f \exp(-i\mathbf{p}_m \mathbf{r}) \right|^2, \quad (3)$$

where $\mathcal{S}(\mathbf{r}) = [1 - \theta(z)\Gamma(\mathbf{b})]$, with z and \mathbf{b} being the longitudinal and transverse coordinates with respect to the direction of the struck nucleon, describes the FSI. In Fig. 2 (left panel) the experimental N_{eff} [13], *viz*

$$N_{eff}(\mathbf{p}_m) = \left[\frac{d^6\sigma}{dE_{e'} d\Omega_{e'} d\mathbf{p}_m} \right]^{exp} \cdot [K(x, Q^2, \mathbf{p}_m) \sigma_{cc1}^{eN}(Q^2, \mathbf{p}_m)]^{-1} \quad (4)$$

is compared with the results of theoretical calculations [5] obtained using (as in all other calculations described in this paper) $\Gamma(\mathbf{b}) = \sigma_{NN}^{tot} [(1 - i\alpha)/(4\pi b_0^2)] \exp(-\mathbf{b}^2/2b_0^2)$. In the right panel of Fig. 2 the Q^2 dependence of the cross section is illustrated for two different values of the azimuthal angle ϕ between the scattering and reaction planes, namely $\phi = 0$

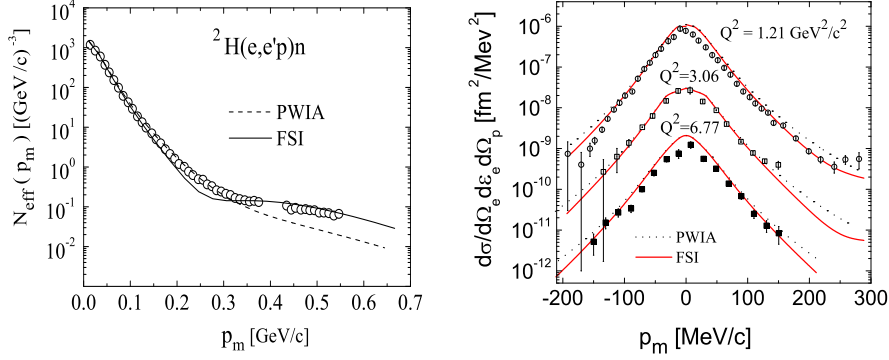


FIG. 2: The process ${}^2\text{H}(e, e'p)n$: comparison between theoretical calculations [5] with the experimental data from JLAB [13] (left) and SLAC [14] (right). The negative values of p_m correspond to protons detected at $\phi = 0$. (After [5]).

(negative values of \mathbf{p}_m) and $\phi = \pi$ (positive values of \mathbf{p}_m). It can be seen that FSI effects lead, in general, to a better agreement with the experimental data.

The processes ${}^3\text{He}(e, e'p){}^2\text{H}$ and ${}^3\text{He}(e, e'p)pn$

In Ref. [5] these processes have been calculated by considering the following three cases:

1. *the PWA approximation*: all particles in the final states are described by plane waves, which means that the transition matrix element is nothing but the three-body ground state wave function in momentum space;
2. *the PWIA approximation*: in this picture (Fig.1a)) the struck proton is always described by a plane wave and the FSI is taken into account only in the (n p) pair of the three-body channel process ${}^3\text{He}(e, e'p)(np)$; in these calculations calculations both the two- and three-body wave functions correspond to the AV18 interaction [19], with the three-body wave function from [2];
3. *the full FSI*: the (n p) system (ground or continuum states) is still described by the exact solution of the Schrödinger equation, whereas the interaction of the struck nucleon with the pair is treated by evaluating the Feynman diagrams of Figs. 1 b) and 1c) within the eikonal approximation. For the three-body channel, one obtains

$$|T_{A,A-1}|^2 \equiv P_D(\mathbf{p}_m, E_m) = \int d\mathbf{k} \quad (5)$$

$$\left| \int d\mathbf{r} d\boldsymbol{\rho} \Psi_{3\text{He}}(\mathbf{r}, \boldsymbol{\rho}) \mathcal{S}^{FSI}(\boldsymbol{\rho}, \mathbf{r}) \exp(i\mathbf{p}_m \boldsymbol{\rho}) \phi_{12}^{\mathbf{k}}(\mathbf{r}) \right|^2 \delta\left(E_m - E_3 - \frac{\mathbf{k}^2}{M_N}\right)$$

where

$$\mathcal{S}^{FSI}(\mathbf{r}_1, \mathbf{r}_2, \mathbf{r}_3) = \prod_{i=1}^2 \left[1 - \theta(z_i - z_3) e^{i\Delta_0(z_i - z_3)} \Gamma(\mathbf{b}_i - \mathbf{b}_3) \right], \quad (6)$$

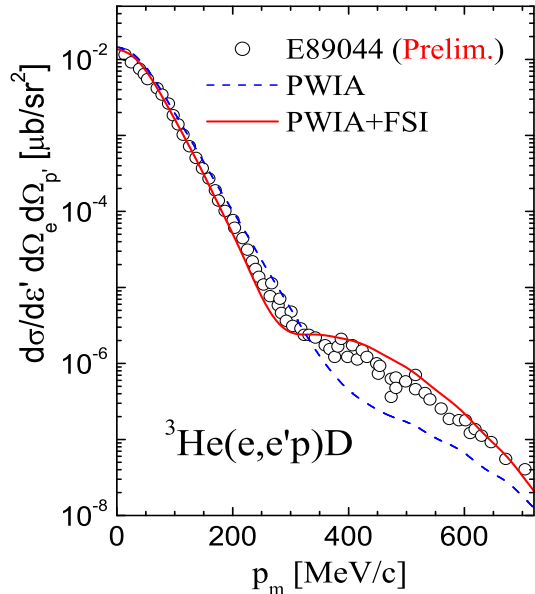


FIG. 3: Comparison of theoretical calculations [5] of the two-body channel process with preliminary experimental data from [15]. AV18 interaction [19]. Three-body wave function from [2]. (After [5]).

Spectral Function, which, when $\Gamma = \Delta_0 = 0$, reduces to the usual one $P(k, E_{rel})$ [7], where $E_{rel} = E_m - E_3$ is the relative energy of the (np) -pair in the continuum and $k \equiv |\mathbf{p}|$ the momentum of the third nucleon.

The results of our calculations are shown in Figs. 3 and 4. Both sets of data refer to the *perpendicular kinematics*, when the final proton is detected almost perpendicularly to \mathbf{p}_m ; it can be seen that in the two-body channel process, the inclusion of FSI effects appreciably improves the agreement with the experimental data.

As for the three-body channel, one sees from Fig. 4 that at sufficiently high values of E_{rel} and p_m , the *PWA* and *PWIA* predictions practically coincide, in agreement with the behaviour of the Spectral Function which, as shown in Fig. 5, exhibits bumps at $E_m \simeq \mathbf{k}^2/(4M_N)$ originating from two-nucleon correlations. Thus, if the PWIA were valid,

In Eq. 6 E_3 is the three-body threshold energy, and $\Delta_0 \sim (q_0/|\mathbf{q}|)E_m$ a factor which arises when the frozen approximation underlying the Glauber approach is released and the recoil momentum of the third nucleon, appearing when the struck nucleon rescatters on the second one, is taken into account [29], [9]. The effects from the factor Δ_0 increase with the removal energy, but in most cases considered they do not appreciably distort the Glauber result (this point is still under investigation [9]). The transition matrix element for the two-body channel has the same form, with the continuum two-body wave function replaced by the deuteron wave function, and the argument of the energy-conserving δ -function properly modified. In eq. 5, $P_D(\mathbf{p}_m, E_m)$ represents the *distorted*

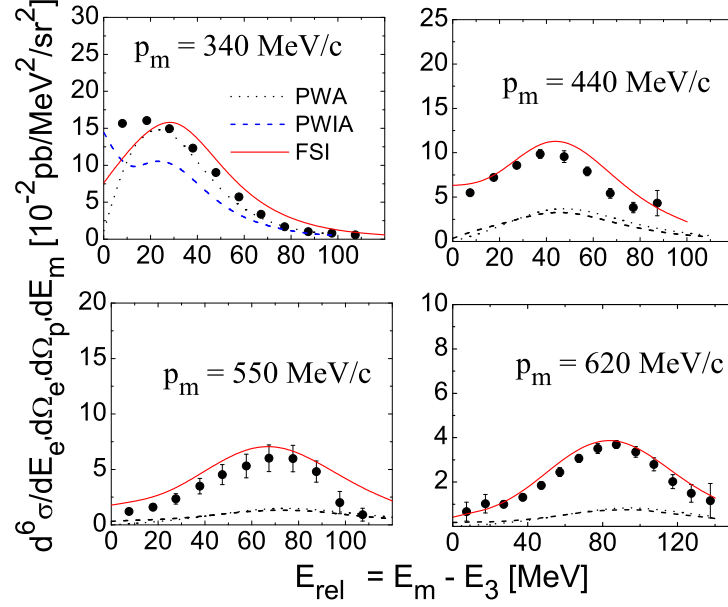


FIG. 4: Comparison of the theoretical calculations [5] of the process ${}^3\text{He}(e, e'p)np$ with preliminary experimental results from [15]. AV18 interaction [19]. Three-body wave function from [2]. (After [5]).

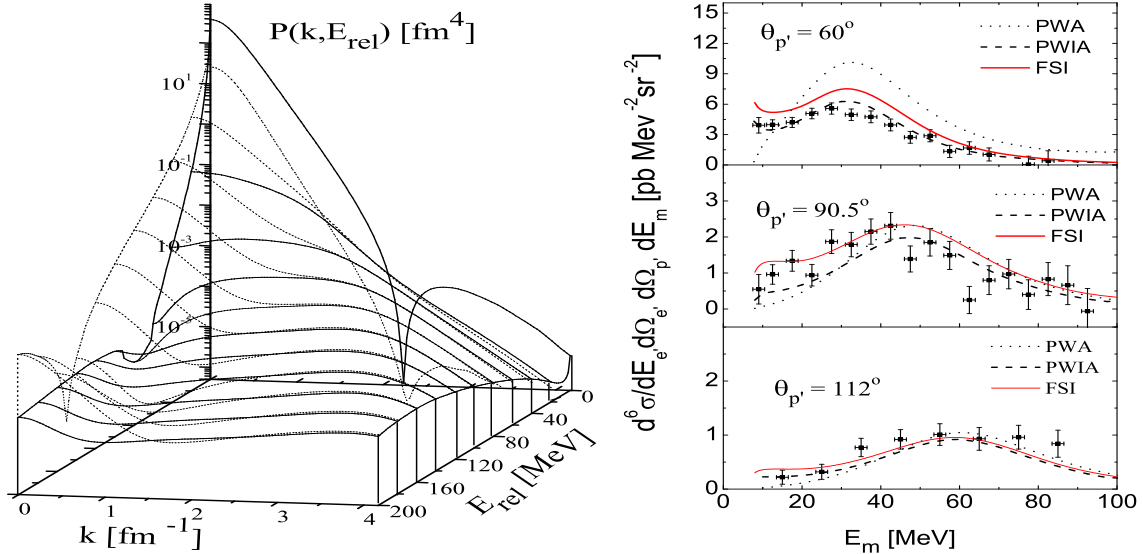


FIG. 5: *Left panel*: the neutron Spectral Function [7] of ${}^3\text{He}$ obtained with the wave functions of Ref. [2] corresponding to the AV18 interaction [19]. E_{rel} is the relative energy of the (pp)-pair and $k \equiv |\mathbf{p}| \equiv k_n$ the momentum of the bound neutron. *Right panel*: comparison of our theoretical calculations (AV18 interaction [19]) of the process ${}^3\text{He}(e, e'p)np$ with the results from [16]. Three-body wave function from [2]. (After [5]).

the ${}^3\text{He}(e, e'p)(np)$ cross section at $p_m \geq 440\text{MeV}/c$ and $E_m \geq 10\text{MeV}$ would be directly related to the three-body wave function. Unfortunately, one sees that in the perpendicular kinematics of [15], the FSI between the struck proton and the (np) pair almost entirely exhausts the cross section. However, as shown in Fig. 5, this does not seem to be the case for the experimental data of [16], where the struck nucleon is detected almost along the direction of \mathbf{p}_m .

The process ${}^3\text{He}(e, e'pp)n$

Extensive theoretical and experimental studies on the $A(e, e'pp)X$ process off complex nuclei have been performed (see e.g. [20–22], and References therein quoted) and the reaction ${}^3\text{He}(e, e'pp)n$ has been investigated at NIKHEF [23] and Jlab [24]. The effects of FSI on this process have been theoretically evaluated in [17] and [7]. In the latter work, the same framework used for the $A(e, e'p)B$ reaction discussed previously has been adopted, and the process has been considered in which γ^* is absorbed by the neutron in ${}^3\text{He}$ and the two protons are emitted by momentum conservation. All of the three particles in the final state are allowed to interact and the three-body final state is described by the following function (spin and isospin variables are omitted for ease of presentation)

$$\psi^f(\mathbf{r}_1, \mathbf{r}_2, \mathbf{r}_3) = S^{FSI}(\mathbf{r}_1, \mathbf{r}_2, \mathbf{r}_3) e^{-i\mathbf{p}_n \cdot \mathbf{r}_3} \phi_{\mathbf{p}_1, \mathbf{p}_2}(\mathbf{r}_1, \mathbf{r}_2) \quad (7)$$

where S^{FSI} , which is given by eq. (6), describes the interaction of the fast neutron “3” with protons “1” and “2”, whose relative wave function $\phi_{\mathbf{p}_1, \mathbf{p}_2}(\mathbf{r}_1, \mathbf{r}_2)$ is the solution of the two-body Schrödinger equation in the continuum. The eight-fold cross section has the following form

$$\frac{d^8\sigma}{dE_{e'} d\Omega_{e'} d\Omega_{\mathbf{p}_n} d|\mathbf{p}_{rel}| d\Omega_{\mathbf{p}_{rel}}} = K(Q^2, \nu, \mathbf{p}_n, \mathbf{p}_{rel}) G_E(Q^2)^2 M(\mathbf{p}_n, \mathbf{p}_{rel}) \quad (8)$$

where

$$M(\mathbf{p}_n, \mathbf{p}_{rel}) = M(|\mathbf{p}_n|, |\mathbf{p}_{rel}|, \theta_1) = \left| \int \psi^f(\mathbf{r}_1, \mathbf{r}_2, \mathbf{r}_3) e^{-i\mathbf{p}_m \cdot \mathbf{r}_n} \psi_{3\text{He}}(\mathbf{r}_1, \mathbf{r}_2, \mathbf{r}_3) \delta\left(\sum_1^3 \mathbf{r}_i\right) \prod_{i=1}^3 d\mathbf{r}_i \right|^2 \quad (9)$$

is the transition form factor, $\mathbf{p}_{rel} = (\mathbf{p}_1 - \mathbf{p}_2)/2$ the relative momentum of the two protons, $\mathbf{p}_m = \mathbf{q} - \mathbf{p}_n = \mathbf{p}_1 + \mathbf{p}_2$, the missing momentum and θ_1 the angle between \mathbf{p}_{rel} and \mathbf{p}_m (as before the spin-isospin variables are not explicitly shown, otherwise a summation over them should appear). The main aim of Ref. [7] was to analyse the problem as to whether

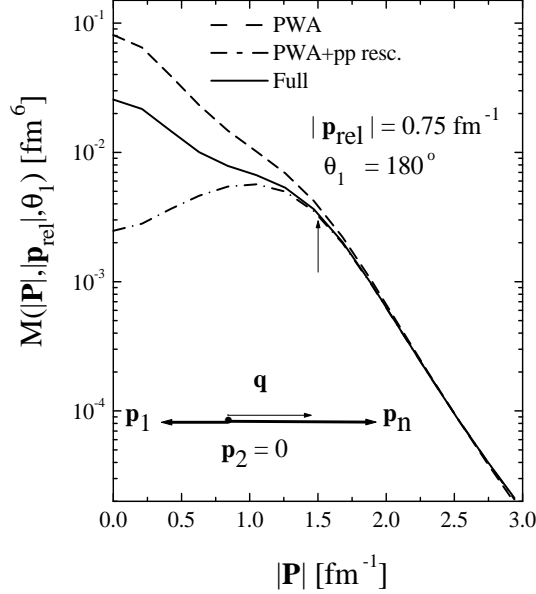


FIG. 6: The effects of the FSI on the ${}^3\text{He}(e, e'pp)n$ process. The transition form factor $M(|\mathbf{p}_n|, |\mathbf{p}_{rel}|, \theta_1)$ (eq. 9), where \mathbf{p}_n is the neutron momentum, $\mathbf{p}_{rel} = (\mathbf{p}_1 - \mathbf{p}_2)/2$ the two-proton relative momentum and $\theta_1 = \widehat{\mathbf{p}_n \cdot \mathbf{p}_{rel}}$, is shown *vs* the missing momentum $\mathbf{P} = \mathbf{p}_1 + \mathbf{p}_2 = \mathbf{q} - \mathbf{p}_n = \mathbf{p}_m$ for fixed values of $|\mathbf{p}_{rel}| = 0.75 \text{ fm}^{-1}$ and $\theta_1 = 180^\circ$ (super-parallel kinematics). **PWA**: all particles in the final state are described by plane waves; **PWIA**: plane wave for the hit neutron plus $p - p$ rescattering; **full**: full three-body rescattering taken into account. The arrow and the momentum vector balance, which refer to the dashed and dot-dashed lines, denote the point corresponding to the Two Nucleon Correlation configuration originating the bumps in the Spectral Function at $\mathbf{k}_n^2/(4M_N) \simeq \mathbf{p}_{rel}^2/M_N$; thus, in the point denoted by the arrow one has $|\mathbf{k}_n| = 2|\mathbf{p}_{rel}| \simeq 1.5 \text{ fm}^{-1}$, $\mathbf{k}_1 \simeq -\mathbf{k}_n$, and $\mathbf{k}_2 \simeq 0$. For $\mathbf{P} > 1.5 \text{ fm}^{-1}$, the ground state momentum balance is always similar to the 2NC configuration ($\mathbf{k}_n \simeq \mathbf{k}_1$, $\mathbf{k}_2 \ll \mathbf{k}_1$), whereas for $\mathbf{P} < 1.5 \text{ fm}^{-1}$, the configuration is far from the 2NC one. AV18 interaction [19]. Three-nucleon wave function from [2]. (After [7]).

proper kinematical conditions could be found where the effects of the FSI are minimized. The results of calculations are shown in Fig. 6, where the transition form factor calculated in the super-parallel kinematics ($\theta_1 = 180^\circ$) is exhibited; in such a kinematics the momenta of the three particles in the continuum lie on the same line. In Fig. 6 the arrow and the momentum vector balance correspond to the kinematical point when $\mathbf{k}_1 = -\mathbf{k}_n$, $\mathbf{k}_2 = 0$ (or $\mathbf{p}_1 + \mathbf{p}_n = \mathbf{q}$, $\mathbf{p}_2 = 0$, having denoted by \mathbf{k} (\mathbf{p}) nucleon momenta before (after) γ^*

absorption). The point, in which $|\mathbf{k}_n| = 2|\mathbf{p}_{rel}|$, corresponds to the two-nucleon correlation (2NC) configuration originating the bumps in the neutron Spectral Function at $E_m = \frac{\mathbf{k}^2}{4M_N}$, shown in Fig. 5. It can be seen from Fig. 6 that right to the 2NC point, the effects from the FSI ($n - (pp)$) and ($(p - p)$) is irrelevant.

The process ${}^4\text{He}(e, e'p){}^3\text{H}$

Recently [11] the effects of color transparency in quasi-elastic lepton scattering off nuclei have been introduced by explicitly considering the finite formation time (FFT) that the hit hadron needs to evolve to its asymptotic physical state. Within the eikonal approach the cross section for the process ${}^4\text{He}(e, e'p){}^3\text{H}$ will depend upon the distorted momentum distributions

$$n_D(\mathbf{p}_m) = \left| (2\pi)^{-3/2} \int d\mathbf{r} \exp(-i\mathbf{p}_m \cdot \mathbf{r}) I(\mathbf{r}) \right|^2 \quad (10)$$

where $I(\mathbf{r})$ denotes the distorted overlap between the ground state wave functions of nuclei A and $(A - 1)$, *viz* (ξ denotes the proper set of Jacobi coordinates)

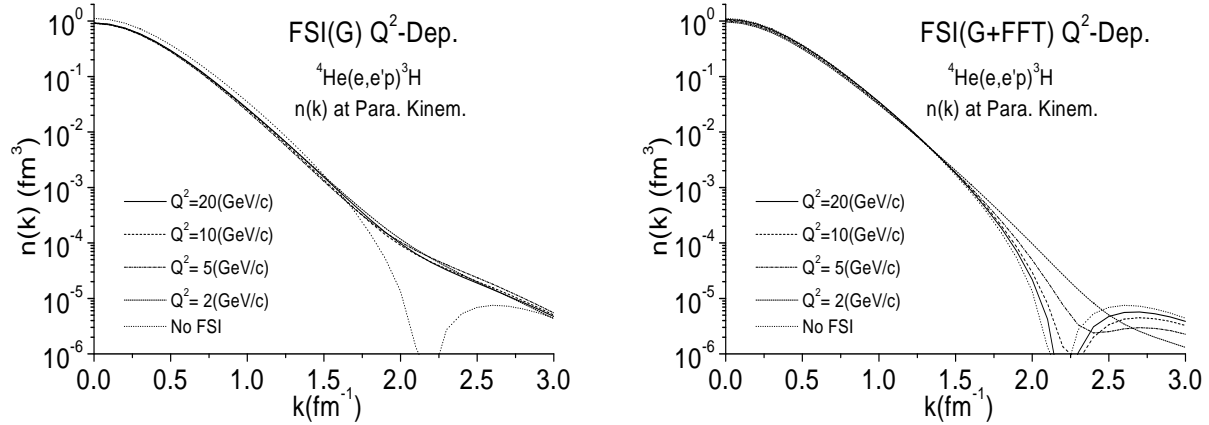


FIG. 7: *Left panel:* the Q^2 dependence of FSI effects calculated within the Glauber approach. *Right panel:* same as in the left panel but with the FFT taken into account. Both Figures refer to parallel kinematics $\theta_{\widehat{\mathbf{qp}_m}} = 0^\circ$. In this Figure $k \equiv |\mathbf{p}_m|$. Four-body wave function from [25]. (After [8])

$$I(\mathbf{r}) = \sqrt{A} \int \psi_{A-1}^*(\xi_{A-1}) \mathcal{S}^{FSI} \psi_A(\xi_A) \prod_{\xi_i} d\xi_i. \quad (11)$$

and

$$\mathcal{S}^{FSI}(\mathbf{r}_1, \mathbf{r}_2, \mathbf{r}_3, \mathbf{r}_4) = \prod_{i=1}^{A-1} G(Ai), \quad G(Ai) = 1 - \theta(z_A - z_i)\Gamma(\mathbf{b}_A - \mathbf{b}_i), \quad (12)$$

is the usual Glauber operator (the hit nucleon is labelled by A). When FFT effects are considered, the $G(Ai)$ can be replaced by [11]

$$G(Ai) = 1 - \mathcal{J}(z_i - z_A)\Gamma(\mathbf{b}_A - \mathbf{b}_i), \quad \mathcal{J}(z) = \theta(z) \left(1 - \exp \left[-\frac{zxM_N M^2}{Q^2} \right] \right), \quad (13)$$

where x is the Bjorken scaling variable, m the nucleon mass, and M represents the average virtuality defined by $M^2 = (m_{Av}^*)^2 - M_N^2$. Eq. 13 shows that at high values of Q^2 FFT effects reduce the Glauber-type FSI, depending on the value of M . In Ref. [8] the value of the average excitation mass m_{Av}^* was taken to be $1.8(GeV/c)$ [11]. the results of calculations are shown in Fig. 7. It can be seen that the exclusive process ${}^4He(e, e'p){}^3H$ at high values of Q^2 could provide a clear cut check of various models which go beyond the treatment of FSI effects in terms of Glauber-type rescattering. A clean and regular Q^2 behaviour leading to the vanishing of FSI effects at moderately large values of Q^2 is predicted and could be validated by the experimental observation of a dip in the cross section at $p_m \simeq 2.2fm^{-1}$. Recently, Benhar *et al* [18] have analyzed the same process, viz. the ${}^4He(e, e'p){}^3H$ reaction, using a colour transparency model. At variance with the results of Ref. [8], their model does not lead to the vanishing of FSI at $Q^2 \simeq 20(GeV/c)^2$. Therefore, it appears that exclusive electron scattering off 4He at high Q^2 would really represent a powerful tool to discriminate various models of hadronic final state rescattering.

III. COMPLEX NUCLEI (Refs. [26–28])

A. Cluster expansion and the nuclear wave function

In the linked-cluster expansion approach developed in Ref. [26–28], the expectation value of a certain operator $\hat{\mathcal{O}}$

$$\langle \hat{\mathcal{O}} \rangle = \frac{\langle \Psi_A | \hat{\mathcal{O}} | \Psi_A \rangle}{\langle \Psi_A | \Psi_A \rangle} \quad (14)$$

is evaluated with correlated wave functions of the following "classical" form

$$\Psi_A = \hat{F}(\mathbf{r}_1, \dots, \mathbf{r}_A) \Phi_A(\mathbf{r}_1, \dots, \mathbf{r}_A), \quad (15)$$

where Φ_A is a mean field (Slater determinant) wave function, and \hat{F} a symmetrized (by the symmetrization operator \hat{S}) correlation operator which generates *correlations* into the mean field wave function; it has the following general form

$$\hat{F} = \hat{S} \prod_{i < j}^A \hat{f}(r_{ij}) \quad (16)$$

with

$$\hat{f}(r_{ij}) = \sum_p f^{(p)}(r_{ij}) \hat{O}_{ij}^{(p)} \quad (17)$$

where the operators $\hat{O}^{(p)}$ are the same which appear in the two-nucleon interaction, having the form (e.g. in case of a $V8$ -type interaction)

$$\hat{O}_{ij}^{p=1-8} = [1, \sigma_i \cdot \sigma_j, S_{ij}, (\mathbf{L} \cdot \mathbf{S})_{ij}] \otimes [1, \tau_i \cdot \tau_j] \quad (18)$$

The central parts $f^{(p)}(r_{ij})$ of the correlation function $\hat{f}^{(p)}$, reflect the radial behaviour of the various components and their actual form is determined either by the minimization of the ground state energy, or by other criteria.

The cluster expansion of Eq.14 is carried out in terms of the quantity $\hat{\eta}_{ij} = \hat{f}_{ij}^2 - 1$, whose integral plays the role of a small expansion parameter; by expanding the numerator and the denominator the terms $\hat{\mathcal{O}}_n$ of the same order n in η_{ij} , are collected obtaining $\langle \hat{\mathcal{O}} \rangle = \mathcal{O}_0 + \mathcal{O}_1 + \mathcal{O}_2 + \dots$, with

$$\begin{aligned} \mathcal{O}_0 &= \langle \hat{\mathcal{O}} \rangle & \mathcal{O}_1 &= \langle \sum_{ij} \hat{\eta}_{ij} \hat{\mathcal{O}} \rangle - \mathcal{O}_0 \langle \sum_{ij} \hat{\eta}_{ij} \rangle \\ \mathcal{O}_2 &= \langle \sum_{ij < kl} \hat{\eta}_{ij} \hat{\eta}_{kl} \hat{\mathcal{O}} \rangle - \langle \sum_{ij} \hat{\eta}_{ij} \hat{\mathcal{O}} \rangle \langle \sum_{ij} \hat{\eta}_{ij} \rangle + \mathcal{O}_0 \left(\langle \sum_{ij < kl} \hat{\eta}_{ij} \hat{\eta}_{kl} \rangle - \langle \sum_{ij} \hat{\eta}_{ij} \rangle^2 \right); \end{aligned} \quad (19)$$

where $\langle [\dots] \rangle \equiv \langle \Phi_A | [\dots] | \Phi_A \rangle$. In Refs. [26–28], the ground-state energy was minimized at various orders of the cluster expansion and the parameters characterizing the correlation functions and the mean-field single-particle wave function have been used in the calculation of the transition matrix elements of various electro-disintegration processes using the same cluster expansion employed to calculate the energy. The ground state energy of ^{16}O and ^{40}Ca has been calculated using the Argonne $V8'$ potential [30] and adopting, as in Ref. [31], the so called f_6 approximation consisting in considering only the first six components of Eq. 17. The expectation value of the Hamiltonian has been obtained by calculating the

average values of the kinetic and potential energies, i.e.

$$\langle \hat{T} \rangle = -\frac{\hbar^2}{2m} \int d\mathbf{k} k^2 n(|\mathbf{k}|), \quad (20)$$

where $n(\mathbf{k})$ is the nucleon momentum distribution,

$$n(|\mathbf{k}|) = \frac{1}{(2\pi)^3} \int d\mathbf{r}_1 d\mathbf{r}'_1 e^{-i\mathbf{k}\cdot(\mathbf{r}_1-\mathbf{r}'_1)} \rho^{(1)}(\mathbf{r}_1, \mathbf{r}'_1), \quad (21)$$

and

$$\langle \hat{V} \rangle = \frac{1}{2} \sum_{i<j} \langle \hat{v}_{ij} \rangle = \frac{A(A-1)}{2} \sum_p \int d\mathbf{r}_1 d\mathbf{r}_2 v^{(p)}(r_{12}) \rho_{(p)}^{(2)}(\mathbf{r}_1, \mathbf{r}_2). \quad (22)$$

The calculations have been performed by cluster expanding the expectation value of the non diagonal one-body, $\hat{\rho}^{(1)}$, and diagonal two-body, $\hat{\rho}^{(2)}(\mathbf{r}_1, \mathbf{r}_2)$, density matrix operators. The six correlation functions $f^{(p)}(r_{ij})$ were the ones obtained in Ref. [31], and the mean field motion has been described by Harmonic Oscillator (HO) and Saxon-Woods (SW) *single particle wave functions* (spwfs). The ground-state energy, the density and the momentum

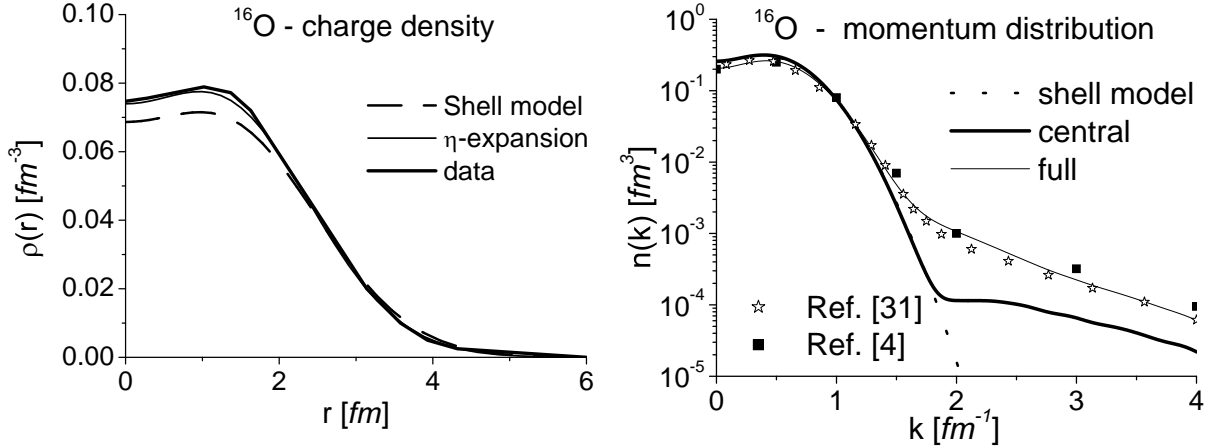


FIG. 8: *Left panel:* the charge density of ^{16}O calculated using the cluster expansion (19) with Harmonic Oscillator (HO) *spwf*. *Dashed line:* mean-field wave results; *full line:* results of the cluster expansion; *thick full line:* experimental data [32]. *Right panel:* the momentum distribution of ^{16}O . *Dotted line:* mean-field result; *full line:* full correlated result; *thick full line:* central correlation only; *open stars:* the FHNC result [31]; *full squares:* the VMC result [4]. The normalization of the density is $4\pi \int \rho(r) r^2 dr = Z$, Z being the number of protons, and the normalization of $n(k)$ is $4\pi \int n(k) k^2 dk = 1$. (After [26])

distribution for ^{16}O and ^{40}Ca have been calculated at first order of the η -expansion and, as in Ref. [31], it has been found that the charge densities corresponding to the minimum

TABLE I: The potential, kinetic and total energies per particle for ^{16}O calculated at 1-st order of the η -expansion ($\mathcal{O}_0 + \mathcal{O}_1$ in Eq. 19). The correlation function and the values of the harmonic oscillator (HO) and Saxon-Woods (SW) parameters are the same as in Ref. [31]. The results from the latter are listed in brackets. (After Ref. [28])

	$\langle T \rangle / A$ (MeV)	$\langle V \rangle / A$ (MeV)	E / A (MeV)
HO	22.4 (22.6)	-26.6 (-27.4)	-4.2 (-4.9)
SW	28.4 (27.3)	-31.5 (-32.4)	-3.1 (-5.1)

of the energy, appreciably disagree with the corresponding experimental quantities; thus, in line with Ref. [31], the mean-field parameters have been changed to obtain agreement between theoretical and experimental charge densities; such a procedure is justified by the mild dependence of the energy around the minimum. Typical results for the energy are shown in Table I. It should be pointed out that the value of the contribution from the seventh and eighth components of the potential have only be estimated. The results for the charge densities and momentum distributions are shown in Figs. 8 and 9. It can be seen that the agreement between the results of the cluster expansion from [26–28] and the FHNC/SOC from [31] appears to be a very satisfactory one. Both approaches predict momentum distributions which do not appreciably differ from the ones obtained in Ref. [4], where the Variational Monte Carlo method and the $AV18$ interaction have been used; the dominant non-central correlations are the isospin, $f_4 = f^{(4)}(r_{ij})\tau_i \cdot \tau_j$, and isospin-tensor,

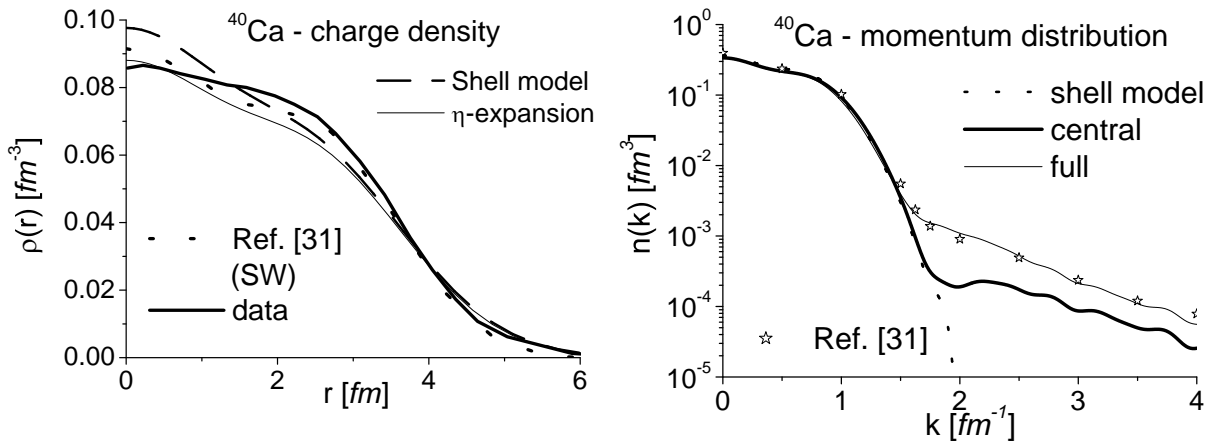


FIG. 9: The same as in Fig. 8, for ^{40}Ca . In the left panel, the additional dotted line was obtained in Ref. [31] with SW spwfs.

$f_6 = f^{(6)}(r_{ij})\tau_i \cdot \tau_j S_{ij}$, correlations. In order to investigate the convergence properties of the momentum distribution the second order cluster contribution to the momentum distribution of ^{16}O has been evaluated ([28]); the results are shown in Fig. 10 and it can be seen that the convergence is very good. The convergence of the energy is being investigated, also by introducing a new cluster expansion which effectively includes higher order terms (see Ref.[26]). A preliminary comparison with the results from Ref. [33] indicates that the value of the kinetic energy for ^{40}Ca is stable, which makes us confident that also the momentum distributions of ^{40}Ca converge at 1st order.

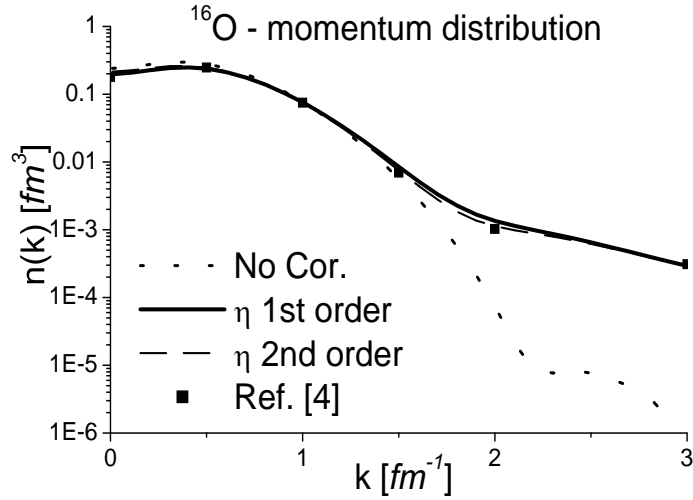


FIG. 10: The nucleon momentum distribution in ^{16}O momentum distributions calculated up to second order in the η -expansion using Saxon-Woods spwfs and the f_1 , f_4 and f_6 correlation functions from [4]. The dotted line represents the mean field result, whereas the dashed (full) line is the result of the cluster expansion at 1st (2nd) order given by $\mathcal{O}_0 + \mathcal{O}_1$ ($\mathcal{O}_0 + \mathcal{O}_1 + \mathcal{O}_2$) in Eq. 19. (After [26])

B. FSI in $A(e, e'p)X$: the Glauber approach

The semi-inclusive $A(e, e'p)X$ process denotes the process in which a summation over all excited states of $(A - 1)$, or, equivalently, over the missing energy $E_m = M_N + M_{A-1} - M_A + E_{A-1}^*$, has been carried out. The cross section (1) becomes then proportional to the *distorted* distorted momentum distributions (see e.g. [34])

$$n_D(\mathbf{p}_m) = (2\pi)^{-3} \int e^{i\mathbf{p}_m(\mathbf{r}_1 - \mathbf{r}'_1)} \rho_D(\mathbf{r}_1, \mathbf{r}'_1) d\mathbf{r}_1 d\mathbf{r}'_1 \quad (23)$$

where

$$\rho_D(\mathbf{r}_1, \mathbf{r}'_1) = \frac{\langle \Psi_A | S^{FSI\dagger} \hat{O}(\mathbf{r}_1, \mathbf{r}'_1) S^{FSI'} | \Psi_A' \rangle}{\langle \Psi_A | \Psi_A \rangle} \quad (24)$$

is the distorted one-body mixed density matrix, S^{FSI} describes the FSI, and the primed

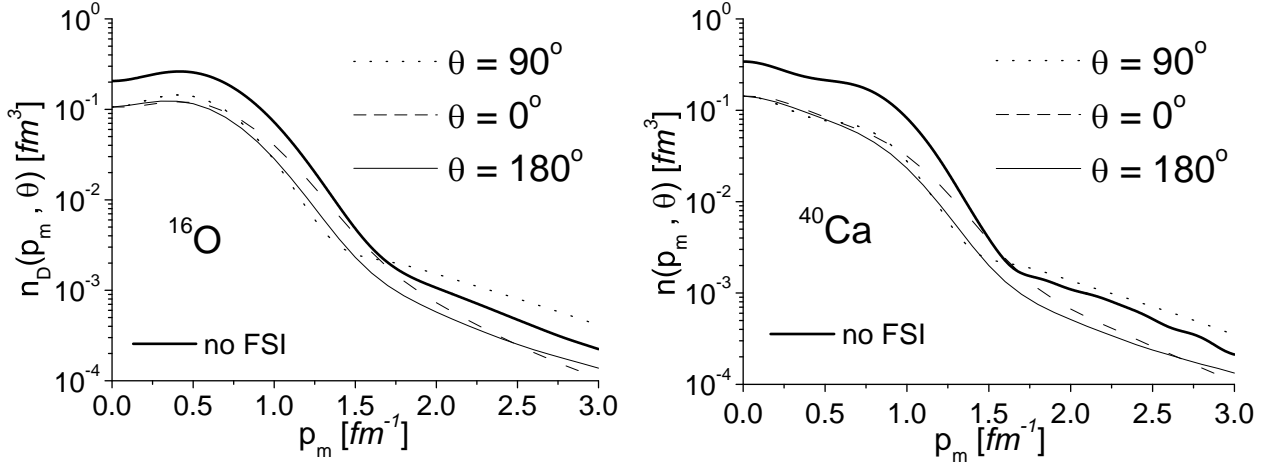


FIG. 11: The distorted momentum distribution, $n_D(\mathbf{p}_m) = n_D(p_m, \theta)$ ($\theta = \widehat{\mathbf{q}}\mathbf{p}_m$), for ^{16}O and ^{40}Ca , obtained from Eq. 23 using correlated wave functions, Harmonic Oscillator *spwfs* and the Glauber operator (26). The value of the integrated nuclear transparency (25) for ^{16}O is 0.5. (After [26])

quantities have to be evaluated at \mathbf{r}'_1 , and \mathbf{r}_i , with $i = 2, \dots, A$. The *nuclear transparency* T is defined as follows

$$T = \frac{\int n_D(\mathbf{p}_m) d\mathbf{p}_m}{\int n(|\mathbf{k}|) d\mathbf{k}} = \int \rho_D(\mathbf{r}) d\mathbf{r} = 1 + \Delta T \quad (25)$$

where $\rho_D(\mathbf{r}) = \rho_D(\mathbf{r}_1 = \mathbf{r}'_1 \equiv \mathbf{r})$ and ΔT originates from the FSI. In Ref. [10] Eq. 23 has been evaluated using a Glauber representation for the operator S , *viz*

$$S^{FSI}(\mathbf{r}_1, \mathbf{r}_2, \dots, \mathbf{r}_A) = \prod_{j=2}^A G(\mathbf{r}_1, \mathbf{r}_j) \equiv \prod_{j=2}^A [1 - \theta(z_j - z_1) \Gamma(\mathbf{b}_1 - \mathbf{b}_j)] \quad (26)$$

where we remind that \mathbf{b}_j and z_j are the transverse and the longitudinal components of the nucleon coordinate $\mathbf{r}_j \equiv (\mathbf{b}_j, z_j)$, $\Gamma(\mathbf{b})$ the Glauber profile function for elastic proton nucleon scattering, and the function $\theta(z_j - z_1)$ takes care of the fact that the struck proton “1” propagates along a straight-path trajectory so that it interacts with nucleon “ j ” only if $z_j > z_1$. The same cluster expansion described in Section II A has been used to evaluate Eq.

25 taking Glauber rescattering exactly into account at the given order n , and using the approximation $|\Psi_{A-3}|^2 = \prod_3^A \rho(i)$. Using such an approach and the mean-field and correlation parameters obtained from the energy calculation, the *distorted* nucleon momentum distributions $n_D(\mathbf{p}_m) = n_D(p_m, \theta)$, where θ is the angle between \mathbf{q} and \mathbf{p}_m , has been obtained in Ref. [26–28]; the results for ^{16}O and ^{40}Ca are presented in Fig. 11.

C. Finite formation time effects

As already discussed in Section II B the effects of color transparency in quasi-elastic lepton scattering off nuclei, can be introduced by considering the finite formation time (FFT) that the hit hadron needs to evolve to its asymptotic physical state. Following Section II B the Glauber factor $G(\mathbf{r}_1, \mathbf{r}_j)$ in Eq. 26 is replaced by

$$G(\mathbf{r}_1, \mathbf{r}_j) = 1 - \mathcal{J}(z_j - z_1)\Gamma(\mathbf{b}_1 - \mathbf{b}_j) \quad (27)$$

with

$$\mathcal{J}(z) = \theta(z) \left(1 - \exp \left[-\frac{zxM_N M^2}{Q^2} \right] \right), \quad (28)$$

where $x = Q^2/(2M_N\nu)$ being the Bjorken scaling variable, and $M^2 = (m_{Av}^*)^2 - M_N^2$ with $m_{Av}^* = 1.8(\text{GeV}/c)$. A suitable quantity for estimating the effect of FSI on the cross section is the *forward-backward* asymmetry, constructed out of forward and backward cross sections,

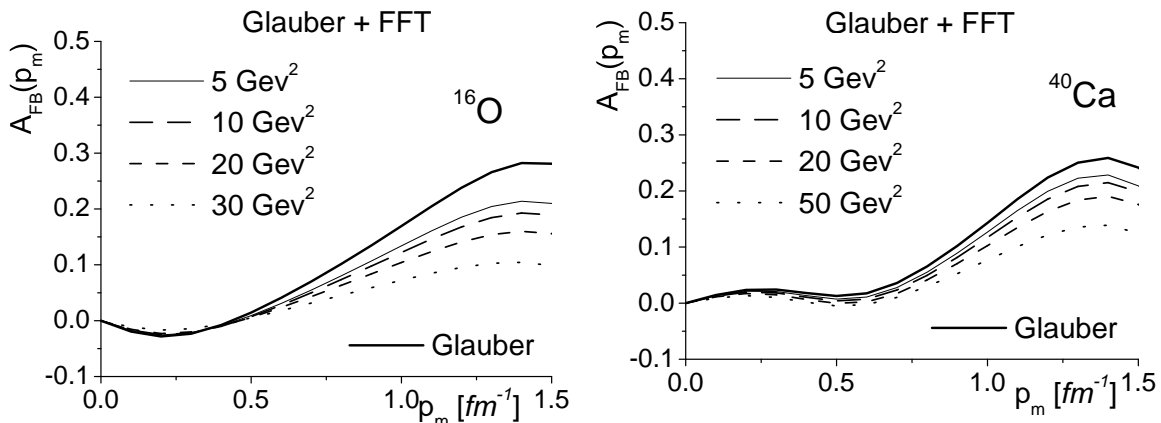


FIG. 12: The forward-backward asymmetry defined by eq. (30), for ^{16}O (left) and ^{40}Ca (right); the thick line represents the Q^2 -independent Glauber result and the other curves include FFT effects. (After [26])

namely

$$A_{FB}(p_m, \theta) = \frac{\sigma(p_m, \theta = 0^\circ) - \sigma(p_m, \theta = 180^\circ)}{\sigma(p_m, \theta = 0^\circ) + \sigma(p_m, \theta = 180^\circ)} \quad (29)$$

Within the factorized approximation for the cross section, A_{FB} reduces to

$$A_{FB}(p_m, \theta) = \frac{n_D(p_m, \theta = 0^\circ) - n_D(p_m, \theta = 180^\circ)}{n_D(p_m, \theta = 0^\circ) + n_D(p_m, \theta = 180^\circ)}; \quad (30)$$

which obviously vanishes in absence of any FSI. The effects of the FSI and the FSI+FFT on A_{FB} are shown in Fig. 12. for ^{16}O and ^{40}Ca for different values of Q^2 ; it can be seen that the inclusion of FFT effects strongly affects the forward-backward asymmetry.

IV. SUMMARY AND CONCLUSIONS

A realistic parameter-free approach aimed at a consistent treatment of initial state correlations and FSI effects in exclusive one- and two-hadron emission processes has been developed, which can be applied both to few- and many-body systems ; in the former case the approach is based upon the use of realistic few-body wave functions, corresponding to realistic interactions, and a generalized eikonal approach, where the Glauber frozen approximation is released. In the case of complex nuclei, reasonable realistic many-body wave functions have been generated by a cluster expansion procedure, which appears to produce densities and momentum distributions of quality comparable to the ones obtained by more advanced many-body approaches. The results obtained for both few- and many-nucleon systems seem to show that by a proper choice of the kinematics, FSI effects might appreciably be reduced, both in one- and two-hadron emissions. Thus it appears that by quasi elastic exclusive processes, the details of the ground-state wave function can eventually be investigated. Preliminary results concerning the generalization of the approach to take into account color transparency effects have been obtained and work is in progress in this direction.

V. ACKNOWLEDGMENTS

The authors are indebted to A. Kievsky for making available the variational three-body wave functions of the Pisa Group and to Giampaolo C3 and Adelchi Fabrocini for providing detailed information on the FHNC/SOC calculation and the numerical values of the

correlation functions. Useful discussions with M. Braun and D. Treleani are gratefully acknowledged. L.P.K. and H. M. are indebted to the University of Perugia and INFN, Sezione di Perugia, for warm hospitality and financial support. This work was partially supported by the Ministero dell'Istruzione, Università e Ricerca (MIUR), through the funds COFIN01.

- [1] W. Glöckle *et al*, *Phys. Rep.* **274** (1996) 107.
- [2] A. Kievsky, S. Rosati and M. Viviani, *Nucl. Phys.* **A551** (1993) 241 and *Private communication*
- [3] S. C. Pieper, R. B. Wiringa, *Ann. Rev. Nucl. Part. Sci.* **51**, 53 (2001)
- [4] S.C. Pieper, R.B. Wiringa and V.R. Pandharipande, *Phys. Rev.* **C46**, 1741 (2000)
- [5] C.Ciofi degli Atti and L.P. Kaptari, invited paper at *International Workshop on Probing Nucleons and Nuclei via the (e, e'p) reaction*, 14-17 october 2003, Grenoble (France), to appear in the Proceedings - `nucl-th/0312043`
- [6] C. Ciofi degli Atti, L.P. Kaptari, D. Treleani, *Phys. Rev C* **63** (2001) 044601
- [7] C. Ciofi degli Atti and L. P. Kaptari, *Phys. Rev.* **C66** (2002) 044004
also in *5th Workshop on Electromagnetically Induced Two-Hadron Emission*, Lund, Sweden, June 2001, Edited by P. Grabmayr.
- [8] H. Morita, M.A. Braun, C.Ciofi degli Atti, D. Treleani and *to appear Nucl. Phys.* **A699**, 328c (2002)
- [9] M. Braun, Ciofi degli Atti, L.P. Kaptari, *Eur. J. Phys.* **A**, in Press
- [10] C.Ciofi degli Atti, D. Treleani *Phys. Rev.* **C60**, 024602 (1999)
- [11] M.A. Braun, C.Ciofi degli Atti, D. Treleani, *Phys. Rev.* **C62**, 034606 (2000)
- [12] T. de Forest Jr, *Nucl. Phys.* **A392** (1983) 232.
- [13] P.E. Ulmer, K.A. Aniol, H. Arenhövel, J.-P. Chen, et al. *Phys. Rev. Lett.* **89** (2002) 062301-1
- [14] H.J. Bulten, P.L. Anthony, R.G. Arnold, E.J. Beise, *Phys. Rev. Lett.* **74** (1995) 4775
- [15] A. Saha, M. Epstein, E. Voutier (spokespersons). TJLAB Experiment E-89-044.
- [16] C. Marchand, M. Bernheim, P. C. Dunn, A. Gérard, *et al*, *Phys. Rev. Lett.* **60** (1988) 1703.
- [17] J. Golak, H.Kamada, H. Witala, W. Glöckle and S. Ishikawa, *Phys. Rev.* **C51** (1995) 1638.
W. Glöckle *et al*, in *5th Workshop on Electromagnetically Induced Two-Hadron Emission*, Lund, Sweden, June 2001, Edited by P. Grabmayr; *Acta Phys. Polonica* **B32** (2001) 3053;

- [18] O. Benhar, N. N. Nikolaev, J. Speth, *et al* Nucl. Phys. **A673** (2000) 241.
- [19] R. B. Wiringa, V. G. J. Stoks, R. Schiavilla, Phys. Rev. **C51** (1995) 38.
- [20] P. Grabmayr, in *Proceedings of the Third International Conference on Perspectives in Hadronic Physics*, edited by S. Boffi, C. Ciofi degli Atti and M. Giannini, Nucl. Phys. **A699** (2002) 41c.
- [21] C. Giusti and F. D. Pacati, Phys. Rev. **C57** (1998) 1691.
- [22] J. Ryckebusch *et al*, Nucl. Phys. **A624** (1997)581.
- [23] D. Groep *et al*. Phys. Rev. Lett. **83** (1999) 5444.
- [24] R. Niyazov, L.B. Weinstein *et al*, nucl-ex/0308013
- [25] H. Morita, Y. Akaishi, O. Endo and H. Tanaka, Prog. Theor. Phys. **78**, (1987) 1117
- [26] M. Alvioli, *PhD Thesis*, Perugia 2003
- [27] M. Alvioli, C. Ciofi degli Atti and H. Morita, invited paper to the *2nd International Conference on Nuclear and Particle Physics with CEBAF at JLab*, Dubrovnik, Croatia, 2003 nucl-th/0309086
- [28] M. Alvioli, C. Ciofi degli Atti and H. Morita, in preparation
- [29] L.L. Frankfurt, W.R. Greenberg, G.A. Miller, M.M. Sargsian, M.I. Strikman, Z. Phys. **A352** (1995) 97;
L.L. Frankfurt, M.M. Sargsian, M.I. Strikman, Phys. Rev. **C56** (1997) 1124
- [30] B.S. Pudliner, V.R. Pandharipande, J. Carlson, S.C. Pieper and R.B. Wiringa, Phys. Rev. **C56**, 1720 (1997)
- [31] A. Fabrocini, F. Arias de Saavedra, G. Co' Phys. Rev. **C61**, (2000) 044302
- [32] H. de Vries, C.W. de Jager and C. de Vries, Atom. Data Nucl. Data Tabl. **36**, 495 (1987)
- [33] A. Fabrocini, F. Arias de Saavedra, G. Co' and P. Folgarait, Phys. Rev. **C57**, (1998) 1668
- [34] N. N. Nikolaev, J. Speth, B. G. Zacharov, JETP **82**, (1996) 1046